

## Electronic Supplementary Information for

### “Molecular Interaction-Dependent Surface Potentials of Sequentially Polymerized Alucone Films”

Ui-Jin Choi,<sup>‡</sup> Hyein Kim,<sup>‡</sup> Yi-Seul Park, Hyemi Lee, and Jin Seok Lee\*

Department of Chemistry, The Research Institute of National Sciences, Sookmyung Women's University, Seoul 140-742, Korea

E-mail: [jinslee@sookmyung.ac.kr](mailto:jinslee@sookmyung.ac.kr)

<sup>‡</sup>These authors contributed equally to this work.

## CONTENTS

- **Experimental Section**
- **Fig. S1** Schematic diagram of homemade hot-wall viscous flow vacuum MLD chamber equipped with an *in situ* QCM measurement system.
- **Fig. S2** Thickness profiles of (a) (TMA/BDO)<sub>100</sub> and (b) (TMA/BYDO)<sub>100</sub> alucone MLD films grown on Si(100) substrate at 120 °C as a function of the dose time of diols, measured by ellipsometry. Their thickness became saturated by self-limiting surface reaction when the dose time of BDO and BYDO exceeded 10 and 60 s, respectively (the TMA dose time was fixed at 10 s).
- **Fig. S3** Two-dimensional AFM images and line profiles of (TMA/BDO)<sub>100</sub> alucone MLD films. The temperatures of BDO precursor were (a) 50 °C and (b) 60 °C, respectively.
- **Fig. S4** The frequency change curve of (a, b) (TMA/BDO)<sub>n</sub> and (c, d) (TMA/BYDO)<sub>n</sub> alucone MLD films for (a, c) early (16 to 20 cycles) and (b, d) late (250 to 255 cycles) stage before converted into mass gains, as shown in Fig. 1 d-g.
- **Fig. S5** Mass gain curve of (TMA/BDO)<sub>3</sub> alucone MLD film was used to define the mass signal, which is represented by an asterisk. Large mass gains were obtained upon exposure to the precursors, such as TMA or diols, resulting from physisorption and chemisorption at the reactive sites of the alucone MLD film on the quartz crystal surface. A gradual decrease in the mass was observed after the purge and evacuation processes due to desorption of the unreacted precursor from the reactive sites of the alucone MLD film.

- **Fig. S6** Most stable location of possible binding sites from DFT calculation. We used two (TMA/BYDO)<sub>1</sub> molecules on the Si(100) substrate and the potential energies for geometrical optimization were (a) -288996.93433, (b) -270094.34005, and (c) -288996.32352 eV; (a) is the most stable binding site for geometry optimization.
- **Fig. S7** FTIR spectra of the (TMA/BDO)<sub>300</sub> and (TMA/BYDO)<sub>300</sub> alucone MLD film on Si(100) substrate. The full width at half maximum (FWHM) values in CH<sub>2</sub> (Asymmetric stretching) peak were 97.33 and 123.69 cm<sup>-1</sup> for (TMA/BDO)<sub>300</sub> and (TMA/BYDO)<sub>300</sub>, respectively.
- **Fig. S8** Two-dimensional AFM images and line profiles of (a) (TMA/BDO)<sub>300</sub> and (b) (TMA/BYDO)<sub>300</sub> alucone MLD films grown on Si(100) wafers. The scan area of each image is 4 μm × 4 μm.
- **Fig. S9** Optimized molecular geometry after double reaction between TMA and two types of diols: (a) BDO and (b) BYDO on Si(100) substrate, obtained from DFT calculation. The potential energies required for double reactions are (a) 1090.70355 eV and (b) 1220.24875 eV for (TMA/BDO)<sub>1</sub> and (TMA/BYDO)<sub>1</sub>, respectively.
- **Fig. S10** Two dimensional AFM images of (a) (TMA/BDO)<sub>100</sub>, (b) (TMA/BYDO)<sub>100</sub>, (c) (TMA/BDO)<sub>300</sub>, and (d) (TMA/BYDO)<sub>300</sub> alucone MLD films grown on Si(100) substrate, which are measured at the same locations as the SKPM images of **Fig. 3**. The RMS roughness values of the (TMA/diol)<sub>n</sub> MLD film are (a) 0.265, (b) 0.142, (c) 0.294, and (d) 0.181 nm, respectively.
- **Table S1.** Sequence of (TMA/diol)<sub>n</sub> alucone MLD reaction process.
- **Table S2.** Average values of surface potential and standard deviation of (TMA/diol)<sub>n</sub> alucone MLD films from 0 to 3 V.
- **Table S3.** Work function of (TMA/diol)<sub>n</sub> alucone MLD films at sample bias 0 V.

## Experimental Section

### Chemicals and Materials.

The inorganic precursor, TMA ( $\text{Al}(\text{CH}_3)_3$ , 97%), and organic precursors (two diols with different carbon bond types, BDO ( $\text{HO}(\text{CH}_2)_4\text{OH}$ ),  $\geq 99\%$  and BYDO ( $\text{HOCH}_2\text{C}\equiv\text{CCH}_2\text{OH}$ ), 99%) were purchased from Sigma-Aldrich Korea (Seoul, South Korea). Isopropyl alcohol (IPA,  $(\text{CH}_3)_2\text{CHOH}$ , 99.5 %) was purchased from Samchun Chemical Co. (Seoul, South Korea). All reagents were used without further purification. Si(100) wafers were purchased from LG Siltron (Seoul, South Korea).

### Preparation of Hydroxyl-terminated Substrate.

The Si(100) wafers were cut into pieces with dimensions of 1 cm (width)  $\times$  1 cm (length), and cleaned by sonication for 2 min in IPA. The Si substrates were then dried using  $\text{N}_2$  gas to remove any particles. The wafer pieces were exposed to plasma treatment for more than 10 min using  $\text{O}_2$  gas to form the hydroxyl-terminated substrate and were loaded into the MLD chamber; the temperature was ramped to 90 or 120  $^\circ\text{C}$  and held there for 30 min.

### Fabrication of Alucone MLD Films.

All of the hybrid organic–inorganic alucone MLD films were fabricated in our homemade hot-wall viscous flow vacuum MLD chamber equipped with an *in situ* QCM (**Fig. S1**). The chamber was heated using a halogen lamp and a heating jacket to produce constant heat at the desired growth temperature; in addition, the line along the gas flow path was controlled with heating tape to prevent precursor condensation. Each precursor was filled in a bubbler for introduction into the vacuum MLD chamber. TMA, the inorganic precursor, was maintained at room temperature because of its sufficient vapor pressure. To induce organic reactions at sufficient vapor pressure of the organic precursors, we changed the temperature of the precursor until the pressure reached 20 mTorr in the MLD chamber. The organic precursors,

BDO and BYDO, were heated to 50 and 70 °C, respectively, to achieve sufficient vapor pressure.

The deposition process sequence for the alucone MLD film is shown in **Table S1**. All the precursors were dosed into the MLD chamber as vapors. After 10 s of TMA dosing, the conditions of the MLD chamber were maintained for 10 s, herein called exposure, to allow the surface reaction to proceed. The gate valve in the pump line was closed to induce sufficient surface reaction during dosing and exposure. The chamber was then purged with Ar at a flow rate of 100 sccm for 120 s to remove residual TMA vapor in the MLD chamber and gas lines, and was then evacuated for 20 s to eliminate particulate contamination of the precursor remaining in the MLD chamber. The dose, exposure, purge, and evacuation sequence was repeated with BDO and BYDO. Each cycle involved binary surface reactions between TMA and the diol, as described in steps 1–8 in **Table S1**.

Growth of the alucone MLD film began from the hydroxylated Si surface, with the MLD reaction proceeding according to **Fig. 1a**. As demonstrated in the schematic illustration, the hydroxylate-terminated surface reacted with TMA to yield a methyl-terminated surface. This surface then reacted with BDO or BYDO, resulting in a hydroxylated surface. MLD was performed by repeating these two reactions in sequence for the desired number of cycles.

#### ***In Situ/Ex Situ* characterization.**

*In situ* QCM measurements (WIZEQCM-1200, WizMac Corp. (Daejeon, South Korea)) were performed in a large viscous flow reactor with a program to monitor and record the mass change signals. The quartz crystal sensors (Inficon Korea Corp. (Seongnam, South Korea)) were quartz crystals with an Au coating and a 6 MHz oscillation frequency. The crystals were installed in the feed-through to prevent material from depositing onto the backside of the crystal surface and faced sideward in the middle of the reactor. Before deposition of the

alucone MLD films, at least 70 cycles of Al<sub>2</sub>O<sub>3</sub> atomic layer deposition were performed on the QCM crystal to create a reproducible starting surface.

The period of the QCM crystal was recorded at 1000 ms intervals, and the mass gain change per unit area according to frequency variation is calculated by below equation (1).

$$\Delta m = \Delta f \cdot (N_q \cdot \rho_q) \cdot f^2 \quad (1)$$

In this equation,  $\Delta m$  = mass gain change per unit area,  $\Delta f$  = frequency variation which is monitored by WizMac software, and  $N_q = 1.670 \times 10^5$  Hz-cm is the frequency constant,  $\rho_q = 2.648$  g/cm<sup>3</sup> is the density of the QCM crystal, and  $f = 6.0 \times 10^6$  is the resonance frequency. The area of QCM crystal is 0.5024 cm<sup>2</sup>. Using this Equation (1), the mass resolution is 6.164 ng/cm<sup>2</sup>.

The refractive index ( $n$ ) and film thickness were measured by *ex situ* ellipsometry (L2W15S830, Gaertner Scientific Corp. (Stamford, U.S.A.)) with a 632.8 nm He-Ne laser. The thickness was measured in at least four spots on each sample to confirm the uniformity of the alucone MLD film.

The surface potential and morphology were simultaneously determined using atomic force microscopy (AFM; NX-10, Park Systems (Suwon, South Korea)) with 160 kHz Au-coated cantilevers using amplitude modulated non-contact AFM (nc-AFM) and scanning Kelvin probe microscopy (SKPM). These images were acquired at 1 mV ac voltage with 17 kHz frequency using a scan size of 4  $\mu\text{m} \times 4 \mu\text{m}$ . A feedback loop was used to vary the DC offset bias to set the  $\omega$  signal of the lock-in amplifier to zero. This value of the DC offset bias provided a measure of the surface potential and the limit of detection was 0.01V.

### **Calculation of Work Function.**

The surface potential was determined by detecting changes in the cantilever deflection caused by an electrostatic force between the tip and the film surface. And it is the contact potential difference (CPD) between the tip and the sample, which could be converted to the work

function difference. The work function of the tip was obtained by using the work function value of HOPG, which is known as 4.65 eV, and measuring the surface potential of HOPG. This value was used for calculation of the work function of the sample. The sample was evaluated under the same conditions used for HOPG and the work functions were calculated using the following equations:

$$\{\text{Work function of tip}\} = 4.65 \text{ eV} + e \cdot \{\text{measured value for HOPG}\} \quad (2)$$

$$\{\text{Work function of sample}\} = -e \cdot \{\text{measured value for sample}\} + \{\text{work function of tip}\} \quad (3)$$

The work function obtained for the tip was 4.745 eV when the surface potential of HOPG from SKPM (0.095 V) was substituted into Equation (2). By using this value and Equation (3), the work function of the sample could be obtained from the surface potential of each sample as determined from SKPM.

### **DFT Calculation.**

All calculations and modeling simulations were conducted with the DMol<sup>3</sup> program of Material Studio 8.0. Geometry optimization was performed with the local density approximation (LDA) using the Perdew-Wang (PWC) functional. We used an all-electron double numerical basis set with the polarization function (DNP). The unit cell structure was simulated with 20 Å of vacuum slab and the Si(100) substrate comprised four layers with 50 atoms. For validation of the optimized molecular geometry of the alucone MLD films, we used one cycle for TMA and BDO or BYDO on the Si(100) substrate.

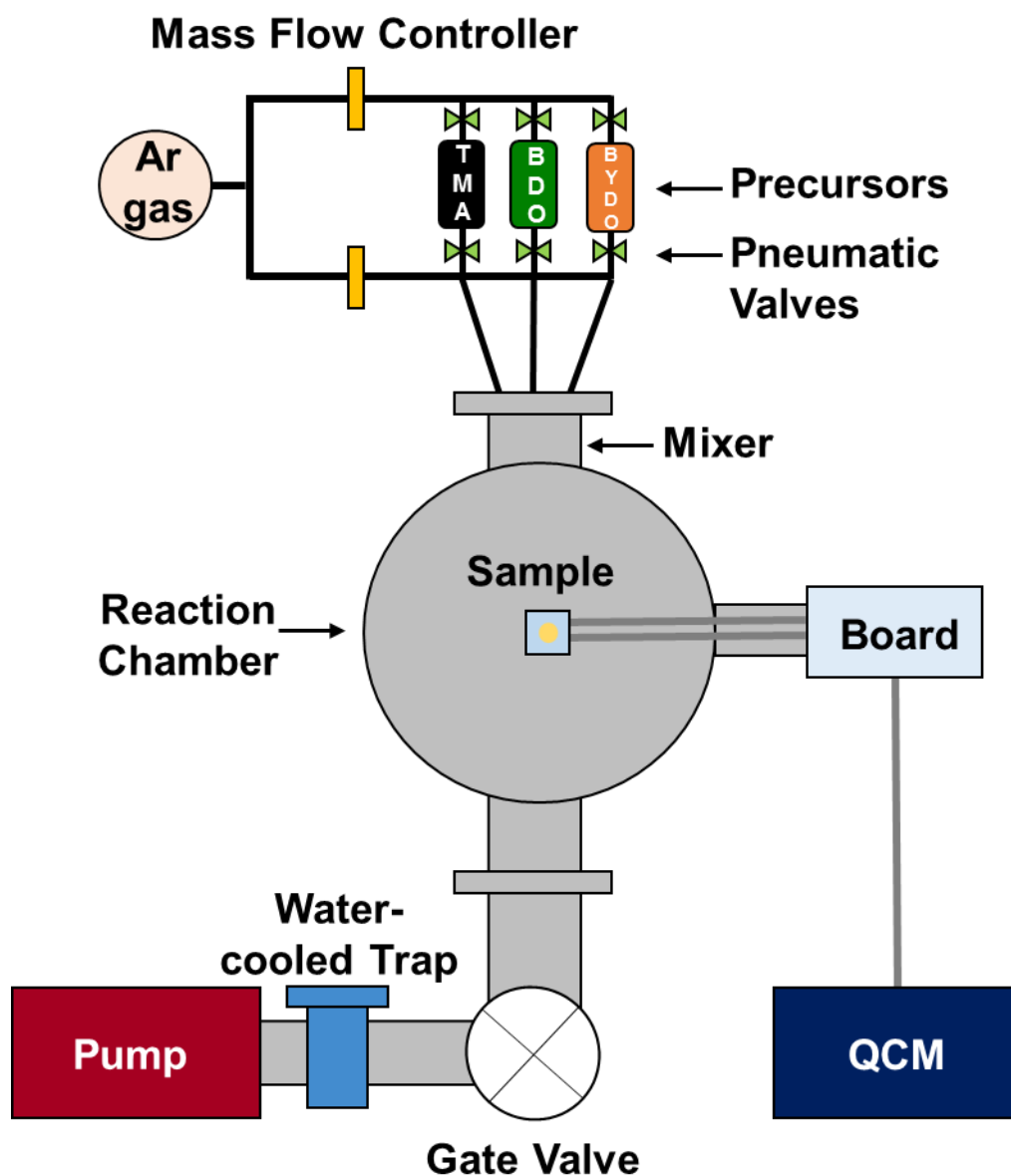


**Fig. S1** Schematic diagram of homemade hot-wall viscous flow vacuum MLD chamber equipped with an *in situ* QCM measurement system.

Sequence	1 <sup>st</sup> Cycle				2 <sup>nd</sup> Cycle	
Step	Step 1	Step 2	Step 3	Step 4	Step 1	...
(TMA/Diol) <sub>n</sub>	TMA dose 10 s	Exposure 10 s	Purge 120 s	Evacuation 20 s	TMA dose 10 s	...
	<b>Step 5</b>	<b>Step 6</b>	<b>Step 7</b>	<b>Step 8</b>	<b>Step 5</b>	...
	BDO dose 10 s or BYDO dose 60 s	Exposure 10 s	Purge 120 s	Evacuation 20 s	BDO dose 10 s or BYDO dose 60 s	...

**Table S1.** Sequence of (TMA/diol)<sub>n</sub> alucone MLD reaction process.

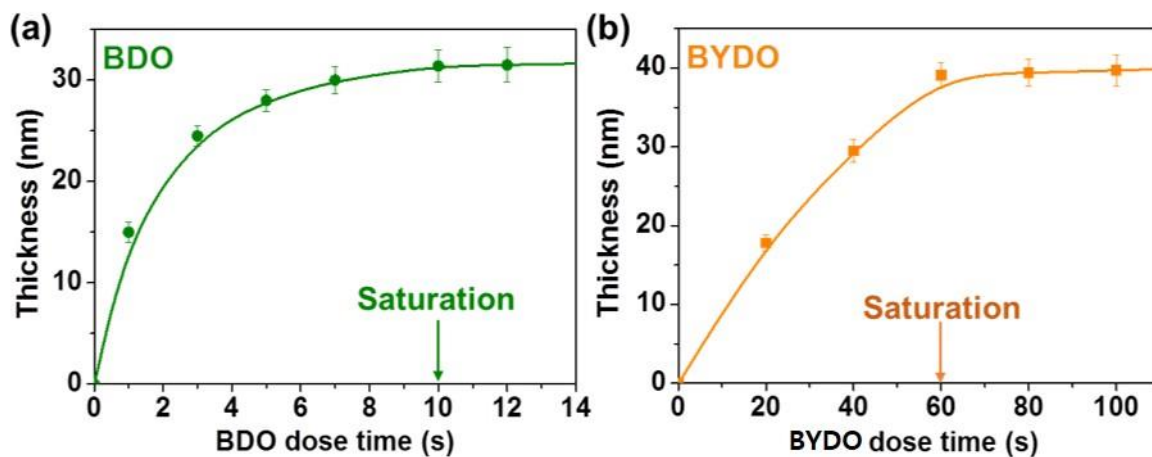


**Fig. S2** Thickness profiles of (a) (TMA/BDO)<sub>100</sub> and (b) (TMA/BYDO)<sub>100</sub> alucone MLD films grown on Si(100) substrate at 120 °C as a function of the dose time of diols, measured by ellipsometry. Their thickness became saturated by self-limiting surface reaction when the dose time of BDO and BYDO exceeded 10 and 60 s, respectively (the TMA dose time was fixed at 10 s).

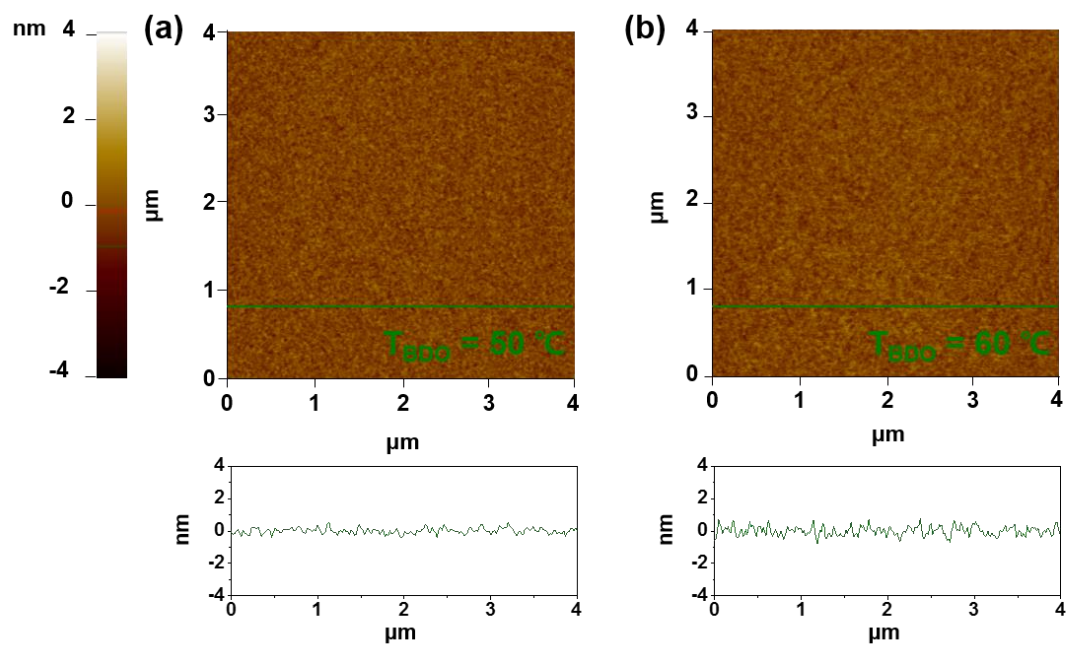


**Fig. S3** Two-dimensional AFM images and line profiles of  $(\text{TMA}/\text{BDO})_{100}$  alucone MLD films. The temperatures of BDO precursor were (a)  $50\text{ }^{\circ}\text{C}$  and (b)  $60\text{ }^{\circ}\text{C}$ , respectively.

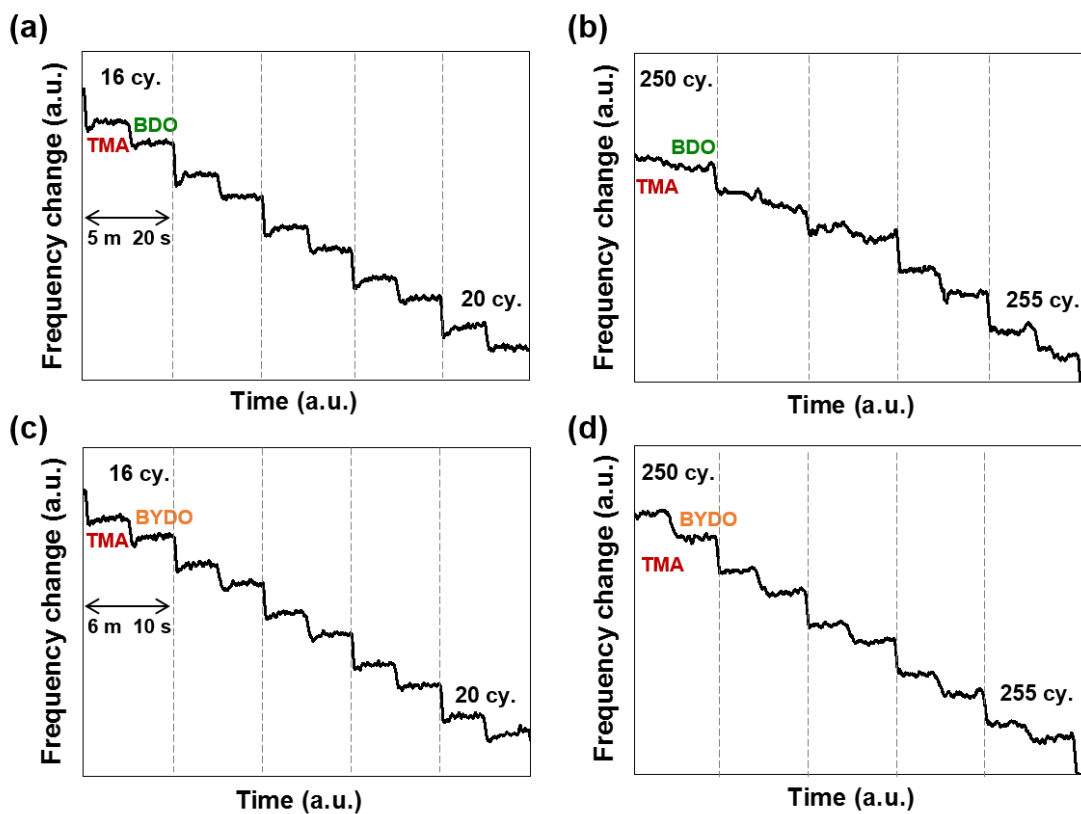


**Fig. S4** The frequency change curve of (a, b)  $(\text{TMA/BDO})_n$  and (c, d)  $(\text{TMA/BYDO})_n$  alucone MLD films for (a, c) early (16 to 20 cycles) and (b, d) late (250 to 255 cycles) stage before converted into mass gains, as shown in **Fig. 1 d-g**.

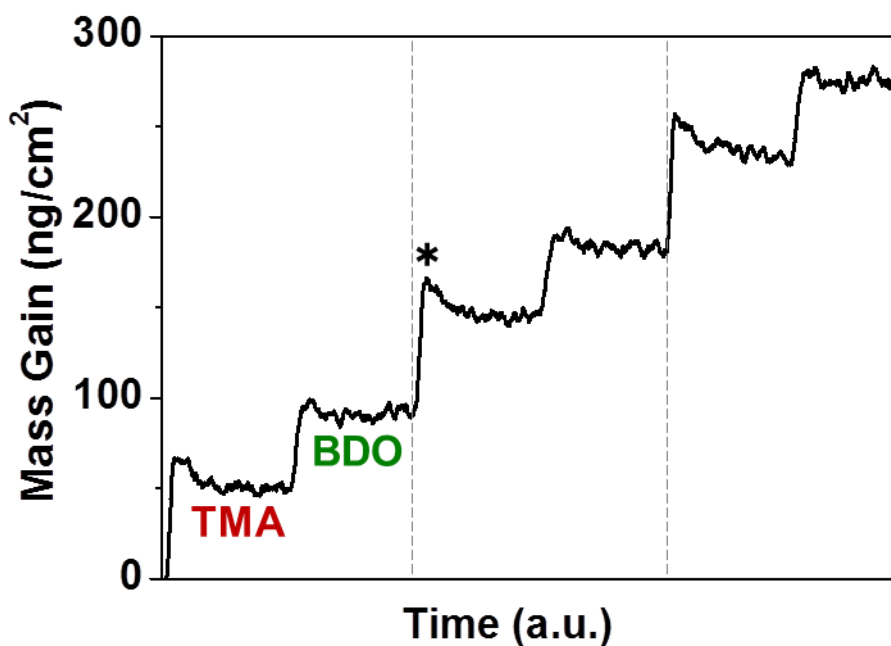


**Fig. S5** Mass gain curve of (TMA/BDO)<sub>3</sub> alucone MLD film was used to define the mass signal, which is represented by an asterisk. Large mass gains were obtained upon exposure to the precursors, such as TMA or diols, resulting from physisorption and chemisorption at the reactive sites of the alucone MLD film on the quartz crystal surface. A gradual decrease in the mass was observed after the purge and evacuation processes due to desorption of the unreacted precursor from the reactive sites of the alucone MLD film.

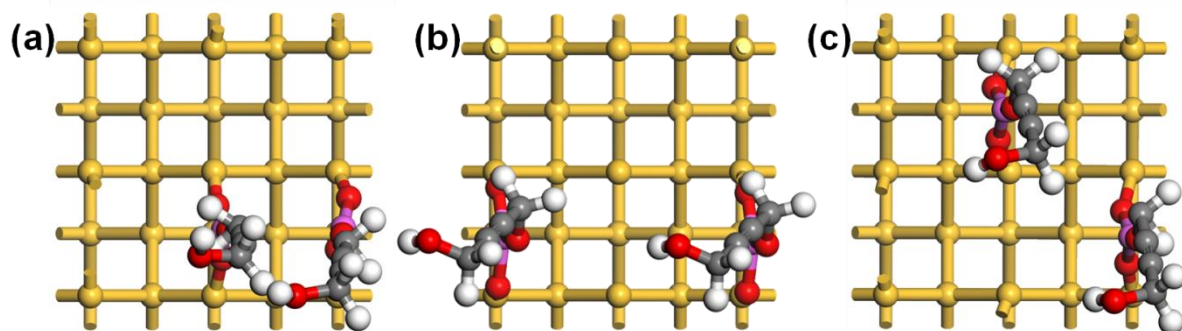


**Fig. S6** Most stable location of possible binding sites from DFT calculation. We used two  $(\text{TMA/BYDO})_1$  molecules on the Si(100) substrate and the potential energies for geometrical optimization were (a)  $-288996.93433$ , (b)  $-270094.34005$ , and (c)  $-288996.32352$  eV; (a) is the most stable binding site for geometry optimization.

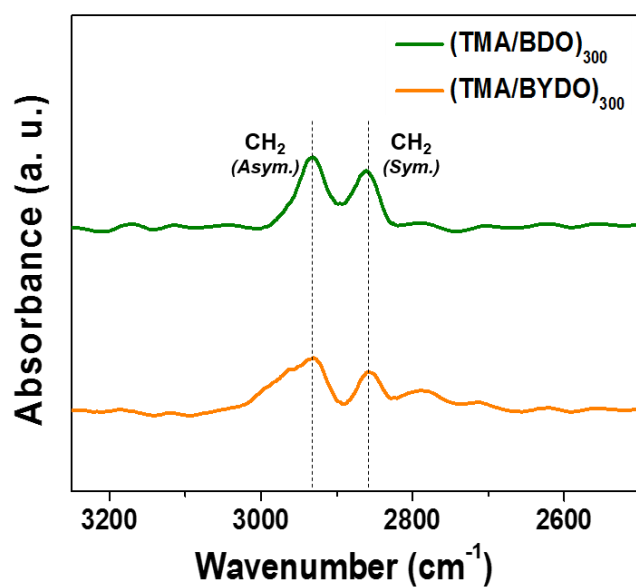


**Fig. S7** FTIR spectra of the (TMA/BDO)<sub>300</sub> and (TMA/BYDO)<sub>300</sub> alucone MLD film on Si(100) substrate. The full width at half maximum (FWHM) values in CH<sub>2</sub> (Asymmetric stretching) peak were 97.33 and 123.69 cm<sup>-1</sup> for (TMA/BDO)<sub>300</sub> and (TMA/BYDO)<sub>300</sub>, respectively.

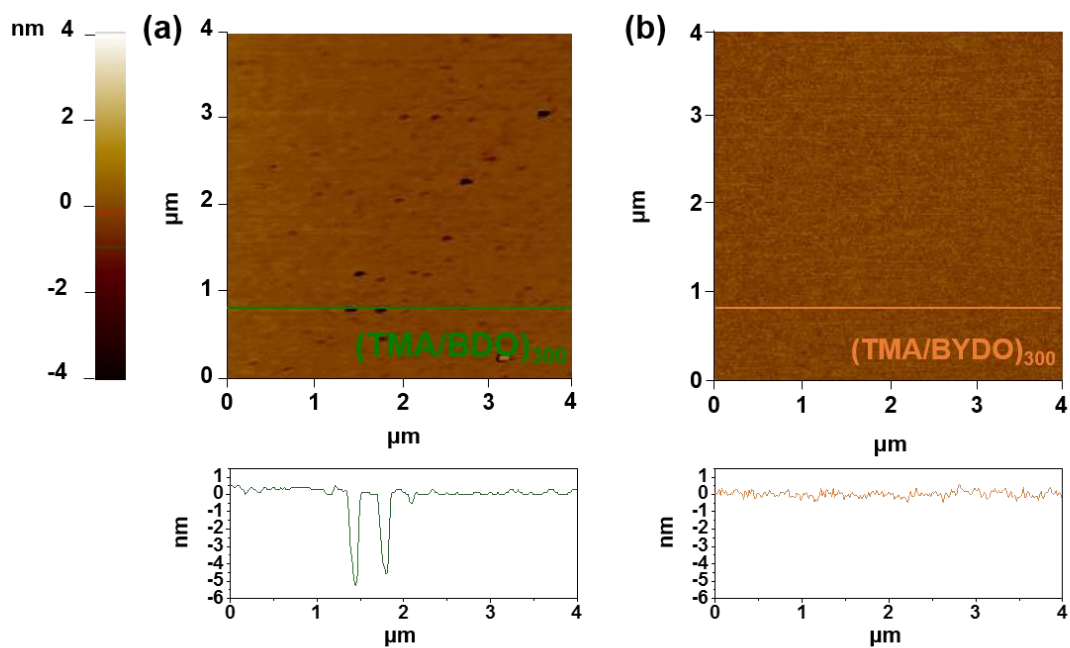


**Fig. S8** Two-dimensional AFM images and line profiles of (a) (TMA/BDO)<sub>300</sub> and (b) (TMA/BYDO)<sub>300</sub> alucone MLD films grown on Si(100) wafers. The scan area of each image is 4 μm × 4 μm.

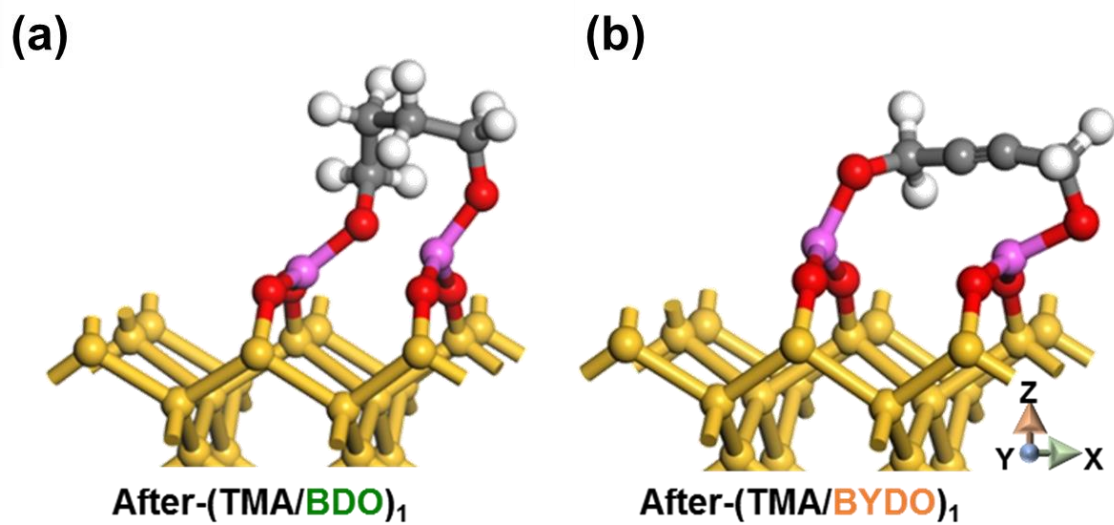


**Fig. S9** Optimized molecular geometry after double reaction between TMA and two types of diols: (a) BDO and (b) BYDO on Si(100) substrate, obtained from DFT calculation. The potential energies required for double reactions are (a) 1090.70355 eV and (b) 1220.24875 eV for (TMA/BDO)<sub>1</sub> and (TMA/BYDO)<sub>1</sub>, respectively.

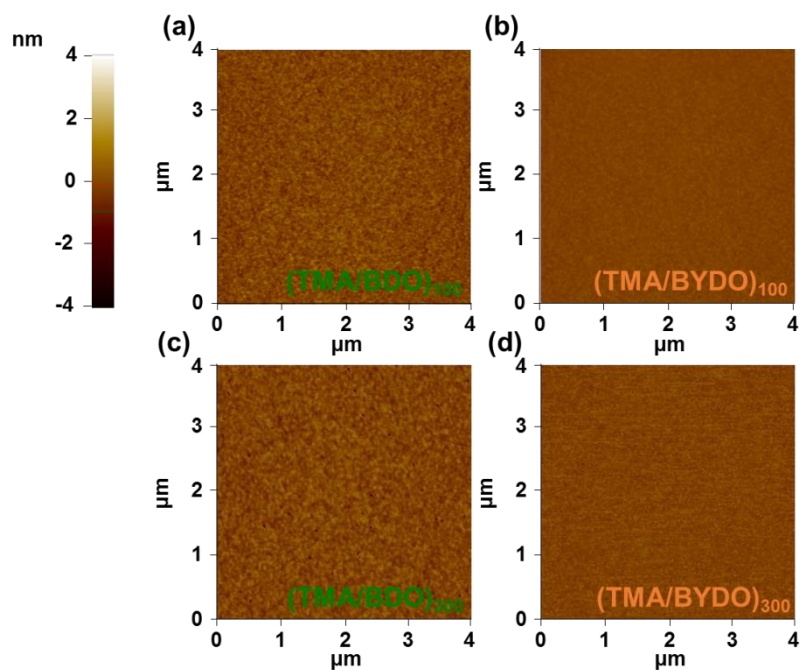


**Fig. S10** Two dimensional AFM images of (a)  $(\text{TMA/BDO})_{100}$ , (b)  $(\text{TMA/BYDO})_{100}$ , (c)  $(\text{TMA/BDO})_{300}$ , and (d)  $(\text{TMA/BYDO})_{300}$  alucone MLD films grown on Si(100) substrate, which are measured at the same locations as the SKPM images of **Fig. 3**. The RMS roughness values of the  $(\text{TMA/diol})_n$  MLD film are (a) 0.265, (b) 0.142, (c) 0.294, and (d) 0.181 nm, respectively.

Potential of Bias (V)	(TMA/BDO) <sub>100</sub>		(TMA/BYDO) <sub>100</sub>		(TMA/BDO) <sub>300</sub>		(TMA/BYDO) <sub>300</sub>	
	Mean (V)	R <sub>q</sub> (V)	Mean (V)	R <sub>q</sub> (V)	Mean (V)	R <sub>q</sub> (V)	Mean (V)	R <sub>q</sub> (V)
0 V	0.598	0.248	0.471	0.048	0.546	0.327	0.470	0.048
1 V	1.601	0.249	1.473	0.049	1.545	0.325	1.468	0.046
2 V	2.597	0.246	2.477	0.049	2.547	0.326	2.463	0.048
3 V	3.586	0.250	3.482	0.048	3.540	0.333	3.480	0.047

**Table S2.** Average values of surface potential and standard deviation of (TMA/diol)<sub>n</sub> alucone MLD films from 0 to 3 V.

Work function(eV)	(TMA/BDO) <sub>100</sub>	(TMA/BDO) <sub>300</sub>	(TMA/BYDO) <sub>100</sub>	(TMA/BYDO) <sub>300</sub>
	4.149	4.199	4.278	4.275

**Table S3.** Work function of (TMA/diol)<sub>n</sub> alucone MLD films at sample bias 0 V.